

Electric Field Gradients in Dilute Alloys of Silver*

C. A. GIFFELS,†† G. W. HINMAN, AND S. H. VOSKO§

Department of Physics, Carnegie Institute of Technology, Pittsburgh, Pennsylvania

(Received August 31, 1960)

The directional correlation of the gamma rays emitted in the decay of Cd^{111} has been measured with the cadmium embedded in the cubic silver lattice in order to observe the electric field gradients produced by various solute atoms. The alloys studied contained small concentrations of cadmium, indium, tin, antimony, or germanium. The results were compared to various theories of screening and were found to be in agreement with a $\cos(2kr + \phi)/r^3$ falloff of shielding charge, where k is the wave number at the Fermi surface. This work corroborates recent results of Rowland by an independent method.

I. INTRODUCTION

THIS paper presents the results of an experiment to determine the nature of the screening charge around a solute atom in a metal. The recent measurements by Rowland¹ of the nuclear resonance signal intensity of copper in dilute copper alloys require for their explanation that the solute atoms produce substantial field gradients at much larger distances than previously expected on the basis of a Thomas-Fermi screening calculation. An explanation of this long-range effect has been put forward by Kohn and Vosko.² They show that the field gradients are due to a redistribution of the conduction electrons and that the long-range effect is a reflection of the sharpness of the Fermi surface. The present work provides an independent corroboration of these results by use of angular correlation techniques.

In this experiment, the angular correlation of gamma rays emitted from Cd^{111} was used as the probe of the field gradients produced by various solute atoms in silver. For this purpose, samples of silver were prepared to which had been added small quantities of other elements. The source of the Cd^{111} was radioactive In^{111} produced within the samples by cyclotron bombardment. After annealing to heal defects, the delayed directional correlation of the gamma rays emitted by the Cd^{111} daughter nucleus was measured. From it the average strength of the electric quadrupole interaction in the vicinity of the solute atom was deduced. The solute elements used were Cd, In, Sn, Sb, and Ge in $\frac{1}{2}$ atomic percent concentration, and Ge also in $\frac{1}{4}$ and $\frac{5}{8}$ atomic percent. The range of effective electric field gradient, as extracted from the measurements, was found to extend beyond ninth nearest neighbors for antimony in silver. This is in good agreement with the theoretical prediction and substantiates Rowland's measurements.

II. EXPERIMENTAL EQUIPMENT AND PROCEDURE

A block diagram of the detecting equipment is shown in Fig. 1. Phototube No. 2 was mounted on a movable platform which rotated about an axis through the source, and was driven automatically between positions at 90° and 180° relative to tube No. 1. A camera automatically recorded the readings of the scalars at the end of each 10-minute counting period, at which time the movable phototube moved to its alternate position, and another 10-minute count commenced.

The alloys were prepared by mixing pellets of 99.99% pure silver with the proper amount of the desired solute in a quartz tube, which was then evacuated and sealed. The tube was then placed in a rocker furnace to melt the pellets and mix the liquid metals. After several minutes of mixing, the alloys were quenched by allowing the tubes to slide out of the furnace into a water bath. Each sample, having a total mass of about 20 grams, was rolled into a sheet 0.013 inch thick. A part of each alloy sheet was sent to the NASA in Cleveland for cyclotron bombardment with 40-Mev alpha particles. The In^{111} , with a half-life of 2.8 days, was produced by the reaction $\text{Ag}^{109}(\alpha, 2n)\text{In}^{111}$. Although other radioactive isotopes were produced, there were no other isomeric levels. Therefore, these isotopes did not affect the experiment because of the delayed coincidence used. Following bombardment, disks $7/32$ inch in diameter were punched from the sheet, sealed in individual evacuated quartz tubes, and annealed for 24 hours at about 925°C . These disks were sub-

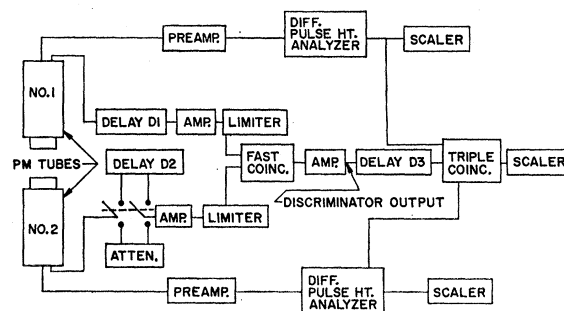


FIG. 1. Block diagram of detecting equipment.

* Supported in part by U. S. Atomic Energy Commission.

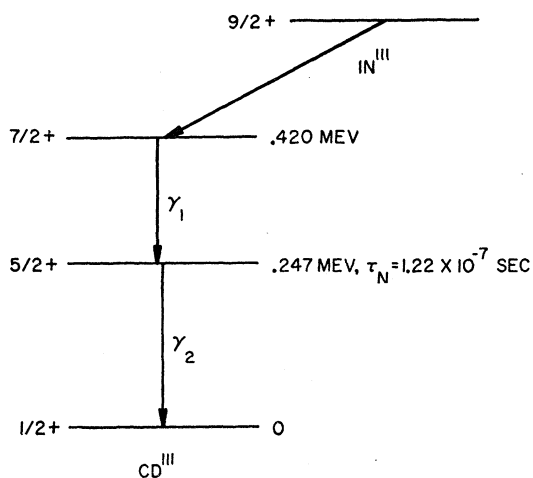
† Portions of this paper were submitted by this author to the Faculty of Carnegie Institute of Technology in partial fulfillment of the requirements for the degree of Doctor of Philosophy.

‡ Now at Bell Telephone Laboratories, Whippany, New Jersey.

§ Now at McMaster University, Hamilton, Ontario, Canada.

¹ T. J. Rowland, *Phys. Rev.* **119**, 900 (1960).

² W. Kohn and S. H. Vosko, *Phys. Rev.* **119**, 912 (1960).

FIG. 2. Simplified decay scheme of In^{111} .

sequently used as sources for the angular correlation measurements.

The decay scheme of In^{111} is shown in Fig. 2. The mean life τ_N of the intermediate state of Cd^{111} has been measured by independent investigators^{3,4} to be 1.22×10^{-7} sec. Phototube No. 1 detected the 0.173-Mev gamma ray, and No. 2 detected the 0.247-Mev gamma, as selected by setting the differential pulse-height analyzers on the corresponding photopeaks in the pulse-height distribution. The resolution of the coincidence circuit is shown in Fig. 3, and was measured using artificial delays with the simultaneous annihilation gamma rays from Na^{22} . Periodically, during the experimental runs, random coincidences were measured by inserting a delay (D_2 in Fig. 1) of 3.6×10^{-7} second.

The use of thin disk-shaped sources was essential to eliminate the need for correction of the measured correlation anisotropy for preferential absorption of the 180° coincidences relative to the 90° coincidences. With the normal to the plane of the source positioned so as to bisect the angle included between the two positions of the movable phototube, the thickness of the source from any point in the source toward the movable detector was the same for either the 180° or 90° position.

Because of the unusual source geometry and uncertain scintillant efficiency function, the correction for finite size of source and scintillant was not accurately calculated. Instead, comparisons were made to measurements using a pure silver source of identical geometry. In this source, no quadrupole interaction is expected if the In^{111} occupies a substitutional position, because of the cubic symmetry of the lattice. A comparison of measurements which were made using various coincidence delays indicates that there is indeed no attenuation of the correlation. It is true that there are other positions in the lattice with cubic symmetry, but the

high annealing temperature makes it very unlikely that In^{111} nuclei occupy them after the annealing.

III. THE AVERAGE ATTENUATION FACTOR

The quantity which is measured in this experiment is the attenuation of the angular correlation due to electric field gradients acting on the Cd^{111} nuclei. In this section we will develop an expression for the average of the attenuation coefficient $G_k(t)$ given by Abragam and Pound.⁵ This average coefficient is related directly to the measured correlation function and depends on the delay time and interval of acceptance of the coincidence resolution curve.

The angular correlation function for the gamma cascade studied here is

$$W(\theta, t) = 1 + A_2 G_2(\omega t) P_2(\cos \theta). \quad (1)$$

The quantity A_2 has been measured⁶ to be -0.180 ± 0.002 . According to Abragam and Pound,⁵ for axially symmetric fields the attenuation coefficient for this isomer is

$$G_2(\omega t) = (7 + 13 \cos \omega t + 10 \cos 2\omega t + 5 \cos 3\omega t) / 35, \quad (2)$$

where t is the delay time between the gamma-ray emissions and ω is the fundamental precession frequency.⁵ Because of the finite resolving time of the coincidence circuit, and the occurrence of different values of ω at different lattice sites in the alloys, the measured correlation function is an average over the

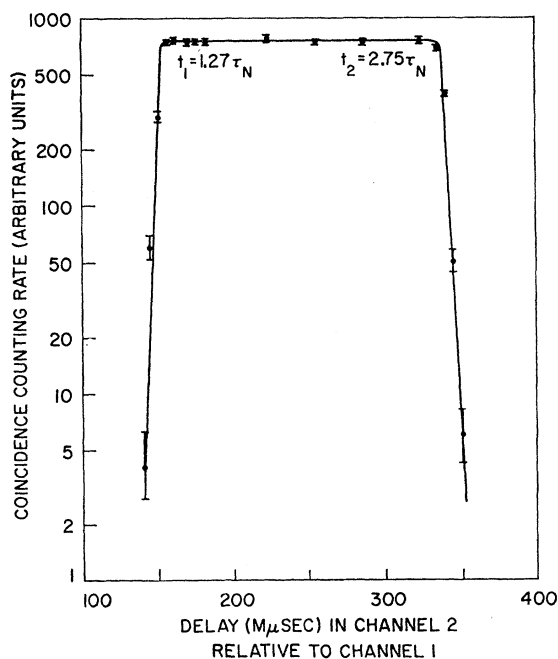


FIG. 3. Coincidence resolution curve.

³ P. C. Simms and R. M. Steffen, Phys. Rev. **108**, 1459 (1957).

⁴ A. Maier and K. P. Meyer, Helv. Phys. Acta **30**, 611 (1957).

⁵ A. Abragam and R. V. Pound, Phys. Rev. **92**, 943 (1953).

⁶ R. M. Steffen, Phys. Rev. **103**, 116 (1956).

resolving time and the various ω 's. The time-integrated correlation function, which still is to be averaged over ω , is

$$\int_{t_1}^{t_2} W(\theta, t) e^{-t/\tau_N} dt / \int_{t_1}^{t_2} e^{-t/\tau_N} dt = 1 + A_2 \bar{G}_2(\omega \tau_N) P_2(\cos \theta), \quad (3)$$

where t_1 and t_2 are the beginning and end of the sensitive time of the coincidence circuit. From Eq. (3)

$$\bar{G}_2(\omega \tau_N) = \frac{1}{e^{-x_1} - e^{-x_2}} \int_{x_1}^{x_2} G_2(\omega \tau_N x) e^{-x} dx, \quad (4)$$

where $x = t/\tau_N$. Figure 4 shows $\bar{G}_2(\omega \tau_N)$ calculated for the values of t_1 and t_2 used in the experiment. The values of t_1 and t_2 were chosen so as to effect a good compromise between sensitivity and counting rate.

Under the assumption that the electric field gradients are due to the solute atoms, the ω in Eq. (4) depends on the relative positions of the solute atoms and the Cd^{111} nucleus. We assume that the major contribution to the electric field gradient at any lattice site comes from the nearest solute atom. The measured average attenuation coefficient can be written

$$\bar{G}_2 = \sum_i P_i \bar{G}_2(\omega^i \tau_N). \quad (5)$$

P_i is the probability that the nearest solute atom occupies a lattice site in the i th shell surrounding the decaying nucleus. $\bar{G}_2(\omega^i \tau_N)$ is given in Fig. 4.

To calculate the P_i 's, we assume the solute atoms and the In^{111} atoms are uncorrelated and occupy random lattice sites. Then if the atomic concentration of solute is c , the probability that there is no solute atom closer to the decaying nucleus than the i th nearest neighbor is

$$r_i = (1-c)^{\sum_{j < i} g_j} \approx \exp[-c \sum_{j < i} g_j], \quad (6)$$

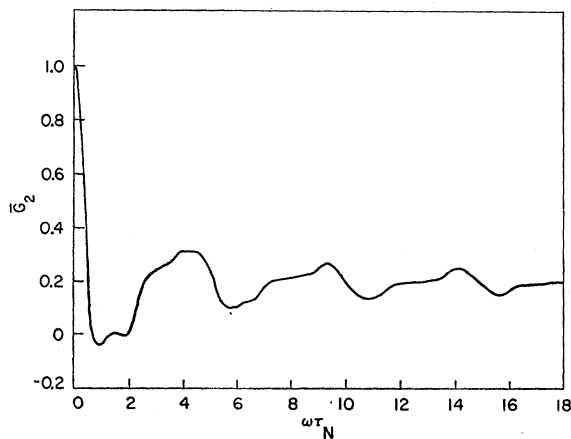


FIG. 4. Attenuation coefficient vs interaction strength for $t_1 = 1.27\tau_N$, $t_2 = 2.75\tau_N$.

TABLE I. P_i is probability that the nearest impurity is an i th nearest neighbor. $P_i^{(1)}$ is the probability that the nearest impurity is an i th nearest neighbor, and there is no other impurity closer than $(i+2)$ th nearest neighbor.

i	g_i	$c=0.0025$		$c=0.005$		$c=0.01$	
		P_i	$P_i^{(1)}$	P_i	$P_i^{(1)}$	P_i	$P_i^{(1)}$
1	12	0.0296	0.0286	0.0582	0.0549	0.1131	0.100
2	6	0.0146	0.0135	0.0279	0.0243	0.0516	0.0393
3	24	0.0556	0.0524	0.1033	0.0917	0.1783	0.140
4	12	0.0266	0.0247	0.0472	0.0406	0.0783	0.0550
5	24	0.0508	0.0483	0.0863	0.0781	0.1243	0.1016
6	8	0.0164	0.0143	0.0265	0.0205	0.0352	0.0210
7	48	0.0912	0.0845	0.1388	0.119	0.1614	0.118
8	6	0.0106	0.00964	0.0151	0.0124	0.0152	0.0103
9	36	0.0607	0.0545	0.0818	0.0662	0.0746	0.0486
10	24	0.0375	0.0343	0.0469	0.0392	0.0367	0.0255
11	24	0.0353	0.0321	0.0416	0.0347	0.0288	0.0201
12	24	0.0333	0.0269	0.0369	0.0241	0.0228	0.0098

where g_j is the number of j th nearest neighbors. Then the probability that the nearest solute atom is in the i th shell is

$$P_i = r_i - r_{i+1}. \quad (7)$$

To check the validity of the assumption that the effect of only the nearest solute atom need be considered, we calculate the probability that there is one solute atom in the i th shell and no other in the next shell or closer. This probability is

$$P_i^{(1)} = n_i c (1-c)^{\sum_{j=1}^{i-1} n_j} - 1 = n_i c r_{i+2} / (1-c). \quad (8)$$

It is seen from the comparison of P_i and $P_i^{(1)}$ in Table I that even for a concentration as high as 1% only one solute atom is important for 70–80% of the decays. In the other 20–30%, the field gradient is of the same order of magnitude, and no serious error results from the simple assumption.

The experimental correlation function for point source and point detectors is expressed in terms of \bar{G}_2 by

$$W(\theta) = 1 + A_2 \bar{G}_2 P_2(\cos \theta). \quad (9)$$

The effect of the finite size of the detectors has been considered by Feingold and Frankel⁷ who show that the measured function is essentially

$$W_M(\theta) = 1 + h_2 A_2 \bar{G}_2 P_2(\cos \theta). \quad (10)$$

For this experiment h_2 is approximately 0.84 ± 0.03 . An estimate⁸ of the effect of the finite source shows that it changes $A_2 \bar{G}_2$ by less than 2%. Expression (10) is used to obtain \bar{G}_2 from the measured correlation function $W_M(\theta)$.

IV. CALCULATION OF FIELD GRADIENTS

A comparison of theory and experiment requires a calculation of ω to evaluate \bar{G}_2 by Eq. (5). The ω is

⁷ A. M. Feingold and S. Frankel, Phys. Rev. 97, 1025 (1955).

⁸ C. A. Giffels, Ph.D. thesis, Carnegie Institute of Technology, Pittsburgh, Pennsylvania, 1960 (unpublished).

related to the electric field gradient at the decaying nucleus by⁵

$$\omega = (3/20)(e^2 Qq/\hbar), \quad (11)$$

where q is a measure of the electric field gradient and is defined by

$$q = (1/e) \left(\frac{\partial^2 V}{\partial z^2} - \frac{1}{3} \nabla^2 V \right). \quad (12)$$

Several calculations^{2,9} of the shielding charge around solute atoms have been made, from which q may be obtained. The result for q is given in terms of an asymptotic series of which the first term is

$$q = \alpha(8\pi/3)\delta n_{\text{free}}(r). \quad (13)$$

$\delta n_{\text{free}}(r)$ is the screening charge density for electrons treated as plane waves, and r is the distance from the solute atom to the decaying nucleus. α is an enhancement factor due to the Bloch nature of the conduction electron wave functions and a polarization of the Cd¹¹¹ core electrons. For large r , δn_{free} may be expressed in terms of the scattering phase shifts η_l for electrons at the Fermi surface as

$$\delta n_{\text{free}}(r) = \frac{A \cos(2kr + \phi)}{r^3}, \quad (14)$$

where k is the Fermi wave number,

$$A = (1/2\pi^2) \left\{ \left[\sum_l (2l+1) \{-\sin\eta_l \cos(\eta_l - l\pi)\} \right]^2 + \left[\sum_l (2l+1) \{-\sin\eta_l \sin(\eta_l - l\pi)\} \right]^2 \right\}^{1/2} \quad (15)$$

and

$$\phi = \tan^{-1} \frac{\sum_l (2l+1) \sin\eta_l \cos(\eta_l - l\pi)}{\sum_l (2l+1) \sin\eta_l \sin(\eta_l - l\pi)}. \quad (16)$$

To evaluate the scattering phase shifts η_l , we use a semiempirical method.² The condition that the excess charge on the solute ion be exactly compensated by a shielding charge of the conduction electrons requires the phase shifts to satisfy the Friedel sum rule¹⁰:

$$Z' = (2/\pi) \sum_l (2l+1) \eta_l, \quad (17)$$

where Z' is the valence difference between solute and solvent.

The residual resistivity of a dilute silver alloy is related to the phase shifts by

$$\Delta\rho = \frac{4\pi\hbar c}{e^2 k} \sum_{l=1}^{\infty} l \sin^2(\eta_{l-1} - \eta_l), \quad (18)$$

where c is the atomic concentration of solute. If it is assumed that only the two phase shifts η_0 and η_1 are important, then Eqs. (17) and (18) are sufficient to determine them. The resulting values of η_0 , η_1 , A , and ϕ are given in Table II. It should be noted that for Cd in Ag the measured resistance is smaller than any

⁹ J. S. Langer and S. H. Vosko, J. Chem. Phys. Solids **12**, 196 (1959).

¹⁰ J. Friedel, Nuovo cimento **7**, 287S (1958).

TABLE II. Scattering phase shifts for solutes in silver with corresponding amplitude and phase of oscillatory electron density.

Solute	Semiempirical method				Perturbation theory	
	η_0	η_1	A	ϕ	A	ϕ
Cd	0.521	0.350	0.0276	0.194	0.0255	π
In	2.656	0.162	0.0456	-0.156	0.0510	π
Sn	2.997	0.572	0.0879	0.517	0.0765	π
Sb	3.441	0.947	0.1118	1.028	0.1020	π
Ge	2.860	0.618	0.0974	0.504	0.0765	π

value obtainable with η_0 and η_1 which satisfy the sum rule (18). The values given in Table II for η_0 and η_1 are those which make $\Delta\rho$ a minimum and are simultaneously consistent with (17). The effect of η_2 has been investigated by use of a screened Coulomb potential. Its effect on A and ϕ is less than 25%.

An approximate calculation of the shielding of a solute atom by the conduction electrons in a metal has been done by Langer and Vosko.⁸ In this method, many-body perturbation theory was applied to calculate the screening charge to first order in the inserted charge $Z'e$. The electrons were treated as a free gas with uniform positive background. The resulting displaced electron density for large r is

$$\delta n(r) = \frac{-2\xi Z' \cos(2kr)}{\pi(4+\xi)^2 r^3}, \quad (19)$$

where $\xi = 2/\pi k a_0$ and a_0 is the Bohr radius. For silver,

$$\delta n(r) = 0.0255 Z' \frac{\cos(2kr + \pi)}{r^3}. \quad (20)$$

The values of A and ϕ obtained from this theory are compared with the semiempirical values in Table II. We see that the two methods give very similar values for the amplitude A which is the critical quantity for comparison with experiment. In comparing with experiment we will use the values obtained from the semiempirical method.

The enhancement factor α in Eq. (13) is defined by

$$\alpha = \int [\phi_{\mathbf{k}}(\mathbf{r}')^2] P_2(\cos\Theta') \frac{1+\gamma(r')}{r'^3} d\mathbf{r}' / \int e^{2i\mathbf{k}\cdot\mathbf{r}'} P_2(\cos\Theta') \frac{1}{r'^3} d\mathbf{r}', \quad (21)$$

where $\phi_{\mathbf{k}}(\mathbf{r}')$ is the Bloch electron wave function at the Fermi surface, \mathbf{k} is in the direction from the solute atom to the point \mathbf{r}' at which q is being evaluated, and Θ' is the angle between \mathbf{r}' and \mathbf{k} . $\gamma(r')$ is the antishielding factor^{11,12} due to the polarization of the core. More than

¹¹ H. M. Foley, R. M. Sternheimer, and D. Tycko, Phys. Rev. **93**, 734 (1954).

¹² R. M. Sternheimer and H. M. Foley, Phys. Rev. **102**, 731 (1956).

one half of the contribution to α comes from the region within 1 Bohr radius of the decaying Cd^{111} nucleus. It is just in this region where it is most difficult to calculate $\phi_{\mathbf{k}}(\mathbf{r}')$ accurately. However, since we are only interested in calculating α to within a factor of 2, we shall calculate it for pure Ag. A partial justification of this procedure is given by the experimental results of Drain¹³ who finds that the Knight shift of Cd in a Ag-Cd alloy is only 13% greater than the Knight shift of Ag in the same alloy. This suggests that the wave function at the Fermi surface in the vicinity of a Ag nucleus is not very different from that in the vicinity of a Cd nucleus. Thus it seems very unlikely that the value of α calculated for pure Ag will be different by more than a factor of 1.5 from the value for Cd in Ag. This accuracy is sufficient for our purposes.

To calculate α for Ag, we require the Bloch wave $\phi_{\mathbf{k}}(\mathbf{r}')$ in the vicinity of a Ag nucleus. For simplicity we approximate $\phi_{\mathbf{k}}$ by a single orthogonalized plane wave:

$$\phi_{\mathbf{k}}(\mathbf{r}') = (1/N^{1/2}) [e^{i\mathbf{k}\cdot\mathbf{r}'} - \sum_{n,l} B_{nl} \psi_{n,l,0}(\mathbf{r}')], \quad (22)$$

where we have taken the polar axis of \mathbf{r}' to coincide with \mathbf{k} . The B_{nl} are coefficients chosen to make $\phi_{\mathbf{k}}$ orthogonal to the normalized atomic core functions $\psi_{n,l,0}$, from which it follows that

$$B_{nl} = \int e^{i\mathbf{k}\cdot\mathbf{r}'} \psi_{n,l,0}(\mathbf{r}') d\mathbf{r}'. \quad (23)$$

For convenience we write

$$B_{nl} = i^l [4\pi(2l+1)]^{1/2} b_{nl}; \quad (24)$$

then the requirement that $\phi_{\mathbf{k}}$ is normalized according to

$$(1/\Omega) \int_{\Omega} |\phi_{\mathbf{k}}(\mathbf{r}')|^2 d\mathbf{r}' = 1, \quad (25)$$

with Ω , the atomic cell volume, gives

$$N = 1 - (3/r_s^3) \sum_{n,l} (2l+1) |b_{nl}|^2, \quad (26)$$

where r_s is the radius of the spherical atomic cell in atomic units and is equal to 3.01 for Ag. The b_{nl} 's have been calculated by numerical integration with Hartree-Fock atomic core functions¹⁴ of Ag^+ . The results are:

$$\begin{aligned} b_{10} &= 0.0127, \\ b_{20} &= -0.0843, & b_{21} &= 0.00325, \\ b_{30} &= 0.321, & b_{31} &= -0.0396, & b_{32} &= 0.00372, \\ b_{40} &= -1.108, & b_{41} &= 0.400, & b_{42} &= -0.173. \end{aligned} \quad (27)$$

¹³ L. E. Drain, *Phil. Mag.* 4, 484 (1959).

¹⁴ B. H. Worsley, *Proc. Roy. Soc. (London)* A247, 390 (1958).

To obtain α as a simple radial integral, we must extract the $P_2(\cos\Theta')$ part of $\phi_{\mathbf{k}}^2$, that is,

$$[\phi_{\mathbf{k}}(\mathbf{r}')^2] = \dots + G(r') P_2(\cos\Theta) + \dots, \quad (28)$$

and substituting in (21) gives

$$\alpha = -\frac{3}{5} \int G(r') \frac{1+\gamma(r')}{r'} dr'. \quad (29)$$

$G(r')$ may be expressed in terms of spherical Bessel functions $j_l(x)$ and the radial part of the Hartree-Fock wave functions $R_{nl}(r')$ by writing

$$\phi_{\mathbf{k}}(\mathbf{r}') = (1/N^{1/2}) \times [e^{i\mathbf{k}\cdot\mathbf{r}'} - \sum_l i^l (2l+1) P_l(\cos\Theta') v_l(r')], \quad (30)$$

where

$$v_l(r') = \sum_n b_{nl} R_{nl}(r'). \quad (31)$$

The resulting expression for $G(r')$ is

$$\begin{aligned} G(r') = & - (1/N) [5j_2(2kr') + 6[v_1(r')]^2 - 12j_1(kr')v_1(r') \\ & + 10v_0(r')v_2(r') - 10j_0(kr')v_2(r') - 10j_2(kr')v_0(r') \\ & - (50/7)v_2(r')^2 + (100/7)j_2(kr')v_2(r') \\ & + 18j_3(kr')v_1(r') - (180/7)j_4(kr')v_2(r')]. \end{aligned} \quad (32)$$

To evaluate α , an estimation of $\gamma(r')$ for Ag^+ was made by use of the results of Foley, Sternheimer, and Tycko¹⁰ for Rb^+ . The contribution to α from the atomic cell is 50, of which approximately 70% comes from the region $r' \leq a_0$. In this region γ is approximately zero. The insensitivity of α to γ is emphasized by noting that if γ were taken to be zero throughout the atomic cell, the contribution to α from the region would be 40 instead of 50. It should also be noted that in the region $r' < a_0$, $G(r')$ is dominated by the term $6[v_1(r')]^2$ of (32). That is, α is essentially determined by the p -wave character of the Bloch wave function in the vicinity of the nucleus. The contribution to α from outside the atomic cell was estimated to be 7. When added to the above this gives $\alpha = 57$ for Ag. The value of α for Cd in Ag is expected to be somewhat larger.

V. COMPARISON OF THEORY WITH EXPERIMENT

The comparison of theory and experiment is made through the quantity \tilde{G}_2 of Eq. (10). To eliminate any errors due to inaccurate geometrical corrections \tilde{G}_2 was obtained by a comparison method. For convenience define

$$R \equiv \frac{W_M(180^\circ)}{W_M(90^\circ)} = \frac{1 + h_2 A_2 \tilde{G}_2}{1 - 0.5 h_2 A_2 \tilde{G}_2} \quad (33)$$

then

$$h_2 A_2 \tilde{G}_2 = 2(R-1)/(R+2). \quad (34)$$

The \tilde{G}_2 for pure Ag should be unity. In order to check this, the calculated value of $h_2 = (0.84 \pm 0.03)$, the measured value⁶ of $A_2 = (-0.180 \pm 0.002)$, and the R found for pure Ag were used to calculate \tilde{G}_2 by (34).

TABLE III. $|\omega^i\tau_N|$ for various solute atoms.

Neighbor	Thomas-Fermi (per unit charge)	Equation (36) with δn_{free} from Table II				
		Cd	In	Sn	Sb	Ge
1	0.950	1.26	2.79	2.34	0.930	2.68
2	0.0866	0.566	1.09	1.32	0.401	1.49
3	0.0145	0.349	0.472	1.18	1.320	1.31
4	0.00340	0.013	0.156	0.205	0.688	0.216
5	0.000962	0.172	0.269	0.518	0.461	0.576
6	0.000306	0.001	0.089	0.104	0.367	0.109
7	0.000106	0.100	0.139	0.331	0.359	0.367
8	0.000040	0.047	0.113	0.069	0.086	0.081
9	...	0.041	0.030	0.183	0.287	0.200
10	...	0.060	0.098	0.172	0.134	0.191
11	...	0.017	0.055	0.0001	0.103	0.004
12	...	0.030	0.026	0.125	0.188	0.138
13	...	0.041	0.066	0.119	0.099	0.133
14	...	0.013	0.002	0.069	0.126	0.075
15	...	0.029	0.040	0.096	0.105	0.106

The result is 0.96 ± 0.04 which provides a confirmation that there are no field gradients present at the decaying Cd^{111} sites. It should be noted that most of the uncertainty in the result is due to h_2 . If we now assume that \tilde{G}_2 for pure Ag is unity, then the uncertainty due to h_2 can be eliminated for the alloy measurements by using ratios. The measured values of \tilde{G}_2 for the various alloys are given in Table IV.

To complete the comparison we calculate from Eq. (5) the \tilde{G}_2 expected according to the theory outlined previously. The frequency corresponding to the nearest solute being in the i th shell, ω^i is obtained by combining Eqs. (11) and (13):

$$\omega^i = \frac{2\pi e^2 Q \alpha}{5 \hbar} \delta n_{free}(r_i) \quad (35)$$

$\delta n_{free}(r_i)$ is obtained from Eq. (14) evaluated at the distance r_i to the i th neighbors. The quantity required in Eq. (5) is $\omega^i\tau_N$, which may be written

$$\omega^i\tau_N = 33.5\alpha Q \delta n_{free}(r_i), \quad (36)$$

with Q in cm^2 and δn_{free} in cm^{-3} .

Estimates^{15,16} of Q range from $0.3 \times 10^{-24} cm^2$ to $10^{-23} cm^2$. However, the latter value is based on a field gradient estimate using an indium metal model of uniform conduction electron distribution and spherically symmetric ions, giving an upper limit on Q . The true value is probably at least a factor 10 smaller.

An alternative to using the above estimates of Q is to compare the quadrupole interactions of Cd^{111*} and of In^{115} , measured in the same environment. This has been done⁸ using the interaction strength for Cd^{111*} measured by Albers-Schönberg *et al.*,¹⁶ and for In^{115} by Hewitt and Knight.¹⁷ If one assumes the electric

¹⁵ H. Narumi and S. Matsuo, *Nuovo cimento* **6**, 398 (1957).

¹⁶ H. Albers-Schönberg, E. Heer, T. B. Novey, and P. Scherrer, *Helv. Phys. Acta* **27**, 547 (1954).

¹⁷ R. R. Hewitt and W. D. Knight, *Phys. Rev. Letters* **3**, 18 (1959).

field gradient at the site of a cadmium nucleus in indium metal is approximately equal to that at an indium nucleus, one obtains $Q_{Cd} = 0.31 Q_{In}$. Using Koster's¹⁸ value for Q_{In} gives $Q_{Cd} = 0.26 \times 10^{-24} cm^2$.

A comparison of the calculated values of $\omega^i\tau_N$ for the above theory and the Thomas-Fermi theory¹⁹ of screening is made in Table III. The value $5 \times 10^{-23} cm^2$ is used for αQ . From Tables II and III in conjunction with Fig. 4 one can calculate \tilde{G}_2 for the various solutes. Table IV gives the measured values of \tilde{G}_2 along with the values predicted by the Thomas-Fermi theory of screening and the recent theory of Kohn and Vosko.² The values of αQ used in Table IV are $5.0 \times 10^{-23} cm^2$ and $1.0 \times 10^{-22} cm^2$. It can be seen from the table that the long-range theory is in agreement with the measured values. The Thomas-Fermi theory cannot explain the results of this experiment. Its inadequacy stems from the fact that only two or three shells of atoms surrounding the solute are affected. On the other hand, the present results require effects as far out as ninth nearest neighbors. It should be noted that due to the uncertainty in α and Q , the product αQ is only known to lie in the range $2 \times 10^{-23} cm^2$ to $1 \times 10^{-22} cm^2$. The theory is in qualitative agreement with experiment for any value in this range.

To determine a lower limit on the range of the oscillations of electron charge density in the vicinity of a solute atom, it is useful to consider the following simplified model.

When a decaying nucleus is within a critical distance r_c of a solute atom, the attenuation coefficient $\tilde{G}_2(\omega^i\tau_N)$ is assumed to be zero, that is the correlation is completely destroyed. However, if the distance to the nearest solute atom is greater than r_c , then $\tilde{G}_2(\omega^i\tau_N)$ is assumed to be unity. The experimental measurements are then used to determine the number of atoms contained within a sphere of radius r_c . It can be seen from Fig. 4 that this simplification is only a crude approximation to the true situation, but it serves to give a lower limit to the number n of lattices sites affected by a single solute atom.

TABLE IV. Comparison of measured and calculated values of G_2 .

Alloy	\tilde{G}_2 (exp)	\tilde{G}_2 (theory)			
		$\alpha Q = 5.0 \times 10^{-23} cm^2$		$\alpha Q = 1.0 \times 10^{-22} cm^2$	
		Thomas-Fermi	Kohn-Vosko	Thomas-Fermi	Kohn-Vosko
$\frac{1}{2}\%$ Cd	0.830 ± 0.031	0.939	0.845	0.937	0.746
$\frac{1}{2}\%$ In	0.713 ± 0.015	0.938	0.802	0.944	0.656
$\frac{1}{2}\%$ Sn	0.627 ± 0.022	0.946	0.649	0.924	0.490
$\frac{1}{2}\%$ Sb	0.534 ± 0.032	0.944	0.586	0.920	0.388
$\frac{1}{2}\%$ Ge	0.843 ± 0.016	0.972	0.780	0.961	0.656
$\frac{1}{2}\%$ Ge	0.688 ± 0.019	0.946	0.631	0.924	0.469
$\frac{3}{8}\%$ Ge	0.620 ± 0.013	0.935	0.573	0.906	0.409

¹⁸ G. F. Koster, *Phys. Rev.* **86**, 148 (1953).

¹⁹ N. F. Mott, *Proc. Cambridge Phil. Soc.* **32**, 281 (1936).

TABLE V. The minimum number n of lattice sites affected by a single solute atom with valence difference Z' and the distortion produced by the solute as measured by $(1/a)da/dc$.

Alloy	Z'	$n = -(1/c) \ln \tilde{G}_2$	$(1/a)da/dc^a$
$\frac{1}{2}\%$ Cd	1	37.2 ± 7.4	0.043
$\frac{1}{2}\%$ In	2	67.6 ± 4.2	0.067
$\frac{1}{2}\%$ Sn	3	93.4 ± 7.0	0.093
$\frac{1}{2}\%$ Sb	4	125 ± 12	0.146
$\frac{1}{4}\%$ Ge	3	68.4 ± 7.6	0.0071
$\frac{1}{2}\%$ Ge	3	74.6 ± 5.5	0.0071
$\frac{3}{8}\%$ Ge	3	76.5 ± 3.4	0.0071

^a Distortion parameter for germanium is taken from W. Hume-Rothery, G. F. Lewin, and P. W. Reynolds, Proc. Roy. Soc. (London) **A157**, 167 (1936); for other solutes, from E. A. Owen and V. W. Rowlands, J. Inst. Metals **66**, 361 (1940).

The probability that there is no solute atom within a radius r_c of the decaying nucleus is

$$f = (1-c)^n, \quad (22)$$

where c is the concentration of solute. Then in this model,

$$\tilde{G}_2 = (1-c)^n$$

and

$$n = \ln \tilde{G}_2 / \ln(1-c) \approx -(1/c) \ln \tilde{G}_2. \quad (23)$$

Table V gives the values of n deduced from the measurements of \tilde{G}_2 . It also shows the relative distortion of the silver lattice by the various solute atoms. The quantity tabulated is

$$(1/a)da/dc,$$

where a is the mean lattice parameter and c is the solute concentration. This quantity is constant over an appreciable range of c . The large number of lattice sites evidently affected by each solute atom cannot be explained by the Thomas-Fermi theory, but it can be understood on the basis of the long-range oscillations in charge density. It is to be emphasized that the numbers n in Table V are lower limits, in view of the

fact that \tilde{G}_2 is not really as small as zero for the majority of the affected lattice sites. (See Fig. 4). For example, if one uses $\tilde{G}_2 = 0.2$ instead of zero for the attenuation coefficient obtained when a solute atom is within a distance r_c , the number of lattice sites affected by the antimony atom is 176 instead of 125. Since 0.2 is a more realistic average for the attenuation coefficient in the region of strong attenuation, the number affected appreciably is probably over 150, which must include atoms as far away as the ninth shell. The constancy of n for the three concentrations of Ge is further confirmation of our interpretation of the experimental results.

VI. CONCLUSIONS

Table V shows that there is a stronger correlation of n with the valence difference Z' than with the distortion parameter $(1/a)da/dc$. Germanium, which distorts the silver lattice very little, nevertheless affects almost as many atoms as tin. This indicates that the major contribution to the electric field gradient at large distances from the solute atom is due to changes in the conduction electron density instead of a distortion of the lattice.

The long-range oscillations in electron density are a consequence of the sharpness of the cutoff of the occupation probability at the Fermi surface. The amplitude of these oscillations would fall off by an additional factor $e^{-(\Delta k)r}$ if the width of the cutoff were Δk . One can estimate from the antimony results, where effects to ninth nearest neighbor are observed, that $\Delta k < 0.09k^0$.

ACKNOWLEDGMENTS

The authors would like to thank Jack Aron and his associates at the Lewis Research Laboratory of the NASA for their generous assistance in making bombardments in their cyclotron. One of the authors (CAG) would like to thank the National Science Foundation for fellowship support.